Optics & Laser Technology 49 (2013) 13–17

Contents lists available at SciVerse ScienceDirect

Optics & Laser Technology

journal homepage: www.elsevier.com/locate/optlastec

Influence of SiO_2 undercoat on the laser-induced damage threshold of 355 nm LaF_3/AlF_3 multilayer reflectors

Xu Li [a,b], Weili Zhang [a,*], Jian Sun [a,b], Yongqiang Hou [a,b], Wenwen Liu [a,b], Kai He [a,b], Chaoyang Wei [a], Kui Yi [a]

[a] Key Laboratory of Materials for High Power Laser, Shanghai Institute of Optics and Fine Mechanics, Chinese Academy of Sciences, Shanghai 201800, China
[b] University of Chinese Academy of Sciences, Beijing 100049, China

ARTICLE INFO

Article history:
Received 9 October 2012
Received in revised form
22 November 2012
Accepted 4 December 2012

Keywords:
Undercoat
Fluoride coatings
Laser-induced damage threshold

ABSTRACT

In the pursuit for 355 nm high laser resistant dielectric coatings, layer-pair number of 10 and 15 LaF_3/AlF_3 high reflectors with and without SiO_2 undercoat were prepared on BK7 substrates. The results indicate considerable increase in 355 nm laser-induced damage threshold (LIDT) for samples with undercoat. The samples were analyzed in Normalized Electric Field Intensity distribution, total stress, damage depth and damage morphology, revealing that SiO_2 undercoat benefits fluoride coatings by shielding substrate defects and reducing coating defects.

1. Introduction

Optical thin film components have always been playing a significant role in high power laser systems [1]. With relatively larger energy band gaps and higher laser-induced damage threshold (LIDT), fluorides are promising coating materials for application in UV lasers [2,3]. However, the major limitations in preparing high LIDT fluoride coatings are crack due to high tensile stress and damage originated from defects. In order to reduce the total stress of fluoride multilayer coatings, research such as ion-assisted deposition (IAD) [2], post-heat treatment [4,5], and oxides/fluorides double stack design [6] were conducted. The dominant defect inside the coatings was considered to be nano-absorbing centers [7–9], and was investigated by planting artificial nanoparticles into the films [10,11].

According to previous research [12] and our work, defects in the substrate–coating interface constitute an important part in defects that reduce LIDT of fluoride coatings, including substrate subsurface defects induced by the polishing process and surface contamination [13] before the coating process [14]. These defects may not only act as initiator of laser-induced damage, but also debase the coatings. SiO_2 undercoat was proved to be effective in shielding substrate interface defects in Ta_2O_5 monolayers [15], but few research has been done on its effects on high-reflective (HR) coatings, especially on fluoride coatings. This work aims at unraveling the influence of substrate etching and SiO_2 undercoat on the LIDT of 355 nm LaF_3/AlF_3 HR coatings.

2. Experimental details

2.1. Sample preparation

10-layer-pair and 15-layer-pair LaF_3/AlF_3 coatings with and without SiO_2 undercoat were prepared on polished BK7 substrates in a Leybold coater equipped with two electron beam guns and Mo boats. LaF_3 and AlF_3 films were deposited by resistant-heating technique, while SiO_2 films were prepared by electron beam deposition (EBD) with substrate temperature of 473 K. A vacuum system containing a cryopump and a Meissner trap was induced to reach the starting pressure of 2.7×10^{-4} Pa. All the substrates were supersonic cleaned and half of them were HF etched in advance to reduce subsurface defects [13,16]. Information for the four designs are listed in Table 1, among which *S*, *H* and *L* refers to a layer with a quarter wavelength optical thickness of each material, respectively.

2.2. Sample characterizations

The transmittance and reflectance spectra of each sample were measured by Perkin–Elmer Lambda 1050 UV/VIS/NIR spectrometer.

The stress of films was obtained using curvature method by measuring the radii of substrates before (R_1) and after (R_2)

* Corresponding author. Tel.: +86 2169918251.
E-mail address: wlzhang@siom.ac.cn (W. Zhang).

0030-3992/$ - see front matter © 2012 Elsevier Ltd. All rights reserved.
http://dx.doi.org/10.1016/j.optlastec.2012.12.005

Table 1
The stack formulas and coating materials for the four designs.

Group	Stack formula	Coating materials
A1	$H(LH)^{10}$	H: LaF_3 [n(355 nm)=1.71]
B1	6S $H(LH)^{10}$	L: AlF_3 [n(355 nm)=1.41]
A2	$H(LH)^{15}$	S: SiO_2 [n(355 nm)=1.54]
B2	6S $H(LH)^{15}$	

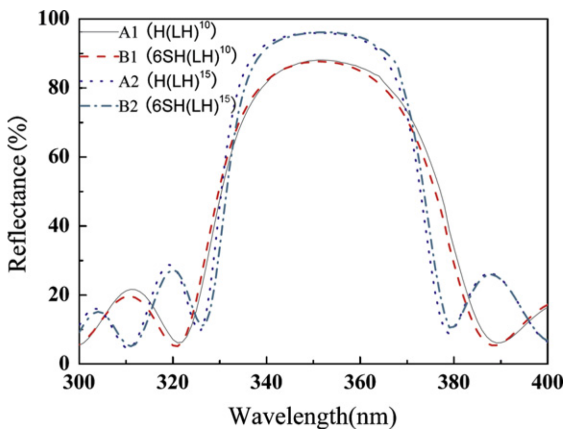

Fig. 1. Reflectance curves for HR coatings with four designs.

deposition. The total stress (σ_{tot}) can be calculated from Stoney's equation [17]:

$$\sigma_{tot} = \frac{E_s}{6(1-\nu_s)}\frac{t_s^2}{t_f}\left(\frac{1}{R_2}-\frac{1}{R_1}\right) \tag{1}$$

where E_s and ν_s refers to Young's modulus and Poisson ratio of substrate, while t_s and t_f represents the thickness of substrate and film, respectively.

The LIDT measurement was performed in the "1-on-1" mode following ISO standard 11254-1.2 on a set-up described in Ref.[6]. The 355 nm, 8 ns illumination laser beam was generated by a tripled Nd:YAG laser system with Gaussian radii of 240/320 μm. The LIDT (J/cm^2) was defined as energy density of the incident pulse when the damage probability was 0%, which could be linearly extrapolated from the corresponding relationship between damage probability and the pulse fluence.

The depth profile of damage sites was obtained by a Veeco optical profiler. The surface defects were observed in dark field mode with magnification of 200 times using a Leica microscope. The damage morphology was observed through a Carl Zeiss Auriga field emission scanning electron microscope (FESEM).

3. Results

3.1. Optical properties

As shown in Fig. 1, the reflectance at 355 nm for the 10-layer-pair (Group 1) and the 15-layer-pair (Group 2) LaF_3/AlF_3 HR coatings reaches 87.2% and 95.8%, respectively, indicating that the reflectance increases with increasing layer pairs. It is also apparent that the SiO_2 undercoat has little influence on the optical performance of the coatings.

3.2. Laser-induced damage threshold

Damage probability curves of coatings on etched substrates are depicted in Fig. 2, from which LIDT was calculated and

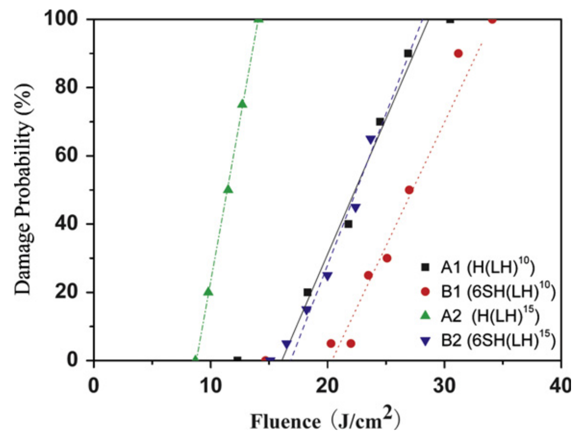

Fig. 2. Damage probability curves for the four designs.

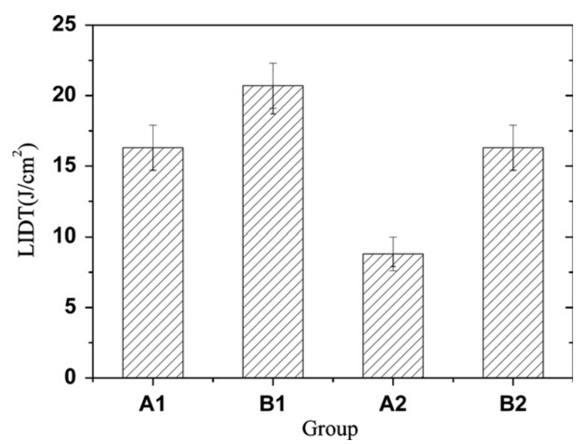

Fig. 3. LIDT values for the four designs (A1: $H(LH)^{10}$, B1: 6S $H(LH)^{10}$, A2: $H(LH)^{15}$ and B2: $6SH(LH)^{15}$).

displayed in Fig. 3. Samples with undercoat (Group B) present considerable improvement in LIDT values than samples without undercoat (Group A).

In Fig. 2, the slope of damage probability curves reflects the density of sensitive defects in the coatings. Compared with $H(LH)^{10}$ high reflectors (A1), $H(LH)^{15}$ coatings (A2) have relatively steeper damage probability, indicating the increasing density of absorption centers. However, the introduction of undercoat reduced the density, resulting in smaller slope in 6S $H(LH)^{15}$ films (B2). Curves of A1 and B1 have similar slope but different intercept, referring to equivalent density of defects and distinct kind of defects. The LIDT resulted in a decline with increasing layer pairs, which will be discussed later.

3.3. Electric field

The normalized electric field intensity (NEFI) inside the coating stack was calculated by thin film design software (TFCalc), as shown in Fig. 4. Because the optical thickness of SiO_2 layer is 6 quarter wavelength, the NEFI remains unchanged with undercoat. The decrease of NEFL from 0.03 (Group 1) to 0.004 (Group 2) due to the additional layer pairs could reveal that the substrate–film interface of Group A was more vulnerable to the incident laser pulse.

3.4. Total stress

As presented in Fig. 5, the tensile stress for group B is relatively smaller than that of group A. This can be attributed to the buffer